

Machine learning for accelerating effective property prediction for poroelasticity problem in stochastic media

Maria Vasilyeva ^{*} Aleksey Tyrylgin [†]

March 1, 2022

Abstract

In this paper, we consider a numerical homogenization of the poroelasticity problem with stochastic properties. The proposed method based on the construction of the deep neural network (DNN) for fast calculation of the effective properties for a coarse grid approximation of the problem. We train neural networks on the set of the selected realizations of the local microscale stochastic fields and macroscale characteristics (permeability and elasticity tensors). We construct a deep learning method through convolutional neural network (CNN) to learn a map between stochastic fields and effective properties. Numerical results are presented for two and three-dimensional model problems and show that proposed method provide fast and accurate effective property predictions.

1 Introduction

Uncertainties remain in most models of real world problems and arise due to lack of knowledge of heterogeneous properties. Uncertainties may be described by stochastic models with uncertain parameters. In the subsurface processes an uncertainty of the properties varying in space. Numerical solution of such problems is difficult and some type of coarsening is necessary to perform fast calculations without resolving small scale heterogeneity by grid. However, most of coarse grid methods are developed for fixed realization of the property field and such coarse grid models may not be sufficient for fast simulations.

Classical numerical methods for solving problems with heterogeneous properties are based on the standard finite element or finite volume approximations. For the applicability and convergence, the size of the computational grid must be small enough to explicitly resolve all the heterogeneity by the grid. Approximation on a fine grid significantly increases the dimension of the discrete problem and requires large computational resources. For such problems, we should use multiscale or upscaling methods to create effective approximations on a coarse grid [31, 33, 6, 7, 32, 3]. For the periodic media, an asymptotic two-scale homogenization

^{*}Institute for Scientific Computation, Texas A&M University, College Station, TX 77843-3368 & Multiscale model reduction laboratory, North-Eastern Federal University, Yakutsk, Republic of Sakha (Yakutia), Russia, 677980. Email: vasilyevadotmdotv@gmail.com.

[†]Multiscale model reduction laboratory, North-Eastern Federal University, Yakutsk, Republic of Sakha (Yakutia), Russia, 677980.

method can be used, where coarse grid (macroscale) equations with effective medium properties are derived. In this method an effective property are calculated for one heterogeneity period by solving local problems [4, 26, 5]. For problems in non-periodic media, the methods of numerical homogenization (upscaling) are used, where local problems are solved to calculate effective characteristics in each local domains. For highly accurate solution a various multiscale methods are developed. Multiscale and homogenization methods assume the solution of local problems for taking into account microscale information for approximation on a macroscale computational grid. Solving such problems are computationally expensive and require calculations for each realization of the property field. Therefore, accelerating of the local calculations is necessary for fast simulations [25, 1, 14, 12, 13, 16].

In recent years, many new highly effective methods for constructing machine learning algorithms are developed. The reason of the increased usage and popularity in recent times associated with development of easy-to-use open source software libraries and availability of graphics processing units (GPUs) for accelerated computation. Furthermore, this jump is associated with development of the deep learning, advance stochastic optimization techniques and robust regularization techniques such as dropout [18, 29, 22, 21]. Deep neural network dramatically improved accuracy of the machine learning methods due to presence of the multiple processing layers that learn representations of data with multiple levels of abstraction (feature extraction) [21]. With the composition of enough layers, very complex functions can be learned. Convolutional neural network is a one particular type of deep network that was much easier to train and generalized much better than networks with full connectivity between layers [20, 21, 27]. The architecture of a convolutional neural network contains composing of the convolutional and pooling layers that passed through a non-linear layers. Several layers of convolution, non-linearity and pooling are stacked, and completes with a several fully-connected layers. The key aspect of deep learning is that these layers of features are not designed by human engineers: they are learned from data using a general-purpose learning procedure. Nowadays, convolutional neural networks have become very popular and are used to solve various problems, including calculation of the physical properties, identifying new dependencies, and solution of the partial differential equations without direct calculations of grid problems [28, 30, 8].

In this work, we construct a machine learning algorithm for an accurate and fast calculations of the effective properties of the random poroelastic media (permeability and elasticity tensors). We develop a machine learning method through a construction of convolutional neural network (CNN) to learn a map between stochastic fields and effective properties. For training convolutional network, we calculate reference effective properties by the solution of the local problems, whereas input data we use a local heterogeneous property on the structured grid (array of pixel values). After that, we use this network to significantly reduce the calculation time of effective characteristics and coarse grid solution of the poroelasticity problem in stochastic media.

The paper is organized as follows. In Section 2, we consider model poroelasticity problem in stochastic media with fine grid approximation. Next, we present a numerical homogenization technique for coarse grid solution in Section 3. In Section 4, we present a machine learning algorithm for accelerating effective property prediction for stochastic poroelastic media. In Section 5, we present numerical results for two and three-dimensional problems for random media with exponential variogram, where we present errors of

numerical homogenization for some test cases, results of the training of the machine learning algorithms, relative errors of algorithm for several samples of realizations. Finally, in Section 5, we present and discuss time of machine learning algorithm construction and prediction time.

2 Model problem

Let p and u are the pressure and displacement. In domain Ω , we consider linear poroelasticity problem for (p, u) [19, 11, 17]

$$\begin{aligned} \frac{1}{M} \frac{\partial p}{\partial t} + \alpha \frac{\partial \operatorname{div} u}{\partial t} - \operatorname{div} \left(\frac{k(x, \omega)}{\nu_f} \operatorname{grad} p \right) &= f, \quad x \in \Omega, \\ -\operatorname{div}(\sigma(u)) + \alpha \operatorname{grad} p &= 0, \quad x \in \Omega, \end{aligned} \quad (1)$$

where C is the elasticity tensor, k is the permeability, σ is the stress tensor, ν_f is the fluid viscosity, f is the source term, M is the Biot modulus and α is the Biot-Willis fluid-solid coupling coefficient and

$$\sigma(u) = C(x, \omega) : \varepsilon(u), \quad \varepsilon(u) = \frac{1}{2} (\operatorname{grad} u + \operatorname{grad} u^T).$$

We note that, k and C are stochastic coefficients and M, α, ν_f are constants. Since the permeability and elastic modulus are a stochastic function, p and u are also stochastic.

Here for two-dimensional case (2D), we have

$$\begin{aligned} u &= (u_1, u_2), \quad \sigma = (\sigma_1, \sigma_2, \sigma_{12})^T, \quad \varepsilon = (\varepsilon_1, \varepsilon_2, \varepsilon_{12})^T, \\ k &= \begin{bmatrix} k_{11} & k_{12} \\ k_{21} & k_{22} \end{bmatrix}, \quad C = \begin{bmatrix} C_{1111} & C_{1122} & C_{1112} \\ C_{2211} & C_{2222} & C_{2212} \\ C_{1211} & C_{1222} & C_{1212} \end{bmatrix}, \end{aligned} \quad (2)$$

and for three-dimensional case (3D)

$$\begin{aligned} u &= (u_1, u_2, u_3), \quad \sigma = (\sigma_1, \sigma_2, \sigma_3, \sigma_{12}, \sigma_{23}, \sigma_{13})^T, \quad \varepsilon = (\varepsilon_1, \varepsilon_2, \varepsilon_3, \varepsilon_{12}, \varepsilon_{23}, \varepsilon_{13})^T, \\ k &= \begin{bmatrix} k_{11} & k_{12} & k_{13} \\ k_{21} & k_{22} & k_{23} \\ k_{31} & k_{32} & k_{33} \end{bmatrix}, \quad C = \begin{bmatrix} C_{1111} & C_{1122} & C_{1133} & C_{1112} & C_{1123} & C_{1131} \\ C_{2211} & C_{2222} & C_{2233} & C_{2212} & C_{2223} & C_{2231} \\ C_{3311} & C_{3322} & C_{3333} & C_{3312} & C_{3323} & C_{3331} \\ C_{1211} & C_{1222} & C_{1233} & C_{1212} & C_{1223} & C_{1231} \\ C_{2311} & C_{2322} & C_{2333} & C_{2312} & C_{2323} & C_{2331} \\ C_{3111} & C_{3122} & C_{3133} & C_{3112} & C_{3123} & C_{3131} \end{bmatrix}. \end{aligned} \quad (3)$$

We consider system of equations (1) with following initial and boundary conditions

$$\begin{aligned} p &= p_0, \quad x \in \Omega, \quad t = 0, \\ p &= p_1, \quad x \in \Gamma_p, \quad \text{and} \quad \frac{\partial p}{\partial n} = 0, \quad x \in \partial\Omega/\Gamma_p, \\ u &= 0, \quad x \in \Gamma_u, \quad \text{and} \quad \sigma \cdot n = 0, \quad x \in \partial\Omega/\Gamma_u. \end{aligned}$$

Variational formulation. We use a finite element method to find an approximate solution of the poroelasticity problem. Let

$$V = \{v \in H^1(\Omega) : v = p_1, x \in \Gamma_p\}, \quad \hat{V} = \{v \in H^1(\Omega) : v = 0, x \in \Gamma_p\}.$$

$$W = \{w \in [H^1(\Omega)]^d : w = 0, x \in \Gamma_u\}, \quad \hat{W} = W.$$

where $d = 2, 3$. We have following variational formulation of the problem: find $(u, p) \in V \times Q$ such that

$$\begin{aligned} d\left(\frac{\partial u}{\partial t}, q\right) + m\left(\frac{\partial p}{\partial t}, q\right) + b(p, q) &= l(q), \quad \forall q \in \hat{Q}, \\ a(u, v) + g(v, p) &= 0, \quad \forall v \in \hat{V}, \end{aligned} \tag{4}$$

where

$$a(u, v) = \int_{\Omega} \sigma(u) : \varepsilon(v) dx, \quad b(p, q) = \int_{\Omega} \frac{k}{\nu_f} \text{grad } p \cdot \text{grad } q dx, \quad m(p, q) = \int_{\Omega} \frac{1}{M} p q dx,$$

$$d(u, p) = \int_{\Omega} \alpha \text{div } u p dx, \quad g(v, p) = \int_{\Omega} \alpha v \cdot \text{grad } p dx, \quad l(q) = \int_{\Omega} f q dx.$$

Fine grid system. Let \mathcal{T}^h is the fine grid partition of the computational domain Ω into finite elements. In particular, we use piecewise linear basis functions for finite element approximation. The standard implicit finite difference scheme is used for the approximation with time step size τ and superscripts $n, n+1$ denote previous and current time levels. We will use fine grid formulation for reference solution and error calculations in Section 5. On the fine grid, the equation (4) can be presented in matrix form:

$$\begin{aligned} D \frac{u^{n+1} - u^n}{\tau} + M \frac{p^{n+1} - p^n}{\tau} + B p^{n+1} &= F, \\ A u^{n+1} + G p^{n+1} &= 0, \end{aligned} \tag{5}$$

where $M = [m_{ij}]$, $m_{ij} = m(\phi_i, \phi_j)$, $B = [b_{ij}]$, $b_{ij} = b(\phi_i, \phi_j)$, $A = [a_{ij}]$, $a_{ij} = a(\psi_i, \psi_j)$, $D = [d_{ij}]$, $d_{ij} = d(\psi_i, \phi_j)$, $G = [g_{ij}]$, $g_{ij} = g(\psi_i, \phi_j)$ and $F = \{f_j\}$, $f_j = l(\phi_j)$, ϕ_i and ψ_i are the linear basis functions defined on \mathcal{T}^h .

3 Numerical homogenization

The size of the computational grids for heterogeneous media must be small enough to explicitly resolve all the heterogeneous by the grid. Approximation on a fine grid significantly increases the dimension of the discrete problem, therefore the computational time, as well as the amount of used memory are also increase. For construction of the coarse grid approximation, we use a numerical homogenization technique, where we solve local problems on a fine grid to identify effective coefficients for each coarse grid cell [31, 10, 15, 24].

Let $\mathcal{T}^H = \cup_i K_i$ ($i = \overline{1, N_c}$) be a structured partition of the computational domain Ω into elements K_i , where N_c is the number of the coarse grid cells and i is the coarse grid cell index. We calculate effective permeability and elastic coefficient, k^* and C^* in each coarse cell for nonperiodic heterogeneous media for some given realization.

Permeability tensor. For calculation of the effective permeability, we solve following local problem in K_i

$$\begin{aligned} -\operatorname{div} \left(k^{K_i}(x, \omega) \operatorname{grad} \psi_j^{K_i} \right) &= 0, \quad x \text{ in } K_i, \\ \psi_j^{K_i} &= x_j, \quad x \text{ on } \partial K_i, \end{aligned} \quad (6)$$

where k^{K_i} is the restriction of the heterogeneous coefficient $k(x, \omega)$ to local domain K_i . Here $x = (x_1, x_2)$ for 2D case and $x = (x_1, x_2, x_3)$ for 3D case. Therefore, for 2D problem, we solve two local problems and for 3D problem, we have three local problems. Note that, another boundary conditions can be applied for local problem.

Next, we can find elements of the effective permeability tensor for current K_i

$$k_{lj}^{*, K_i}(\omega) = \frac{1}{|K_i|} \int_{K_i} k^{K_i}(x, \omega) \frac{\partial \psi_l^{K_i}}{\partial x_j} dx, \quad l, j = \overline{1, d}, \quad (7)$$

where d is problem dimension, $d = 2$ or 3 . This permeability tensor is symmetric.

Elasticity tensor. For effective elastic modulus, we apply similar algorithm and solve following local problem in K_i

$$\begin{aligned} -\operatorname{div}(C^{K_i}(x, \omega) : \varepsilon(\phi_{rs}^{K_i})) &= 0, \quad x \text{ in } K_i, \\ \phi_{rs}^{K_i} &= \Lambda^{(rs)} x, \quad x \text{ on } \partial K_i, \end{aligned} \quad (8)$$

where $\phi^{K_i} = (\phi_1^{K_i}, \phi_2^{K_i})$ for $d = 2$, $\phi^{K_i} = (\phi_1^{K_i}, \phi_2^{K_i}, \phi_3^{K_i})$ for $d = 3$ and

$$\Lambda_{ij}^{(rs)} = \frac{1}{2} (\delta_{ir} \delta_{js} + \delta_{is} \delta_{jr}), \quad r, s = \overline{1, d}.$$

The elements of the effective elastic modulus are calculated as follows

$$C_{rspq}^{*, K_i}(\omega) = \frac{1}{|K_i|} \int_{K_i} C(x, \omega) \varepsilon(\phi^{(rs)}) : \varepsilon(\phi^{(pq)}) dx, \quad r, s, p, q = \overline{1, d}. \quad (9)$$

This elasticity tensor is symmetric.

There are existed several approaches for the numerical homogenization methods based on the two-scale asymptotic analysis with solution of the local problems in representative volume K_i with periodic boundary condition, Dirichlet or Neumann boundary condition, or mixed boundary condition.

Coarse grid system. Finally, we solve the poroelasticity problem on a coarse grid with precalculated effective permeability and elastic modulus

$$\begin{aligned} \frac{1}{M} \frac{\partial p}{\partial t} + \alpha \frac{\partial \operatorname{div} u}{\partial t} - \operatorname{div} \left(\frac{k^*(x, \omega)}{\nu_f} \operatorname{grad} p \right) &= f, \\ -\operatorname{div}(C^*(x, \omega) : \varepsilon(u)) + \alpha \operatorname{grad} p &= 0, \end{aligned} \quad (10)$$

using Galerkin finite element method. We note that, for each random field realization, we should calculate effective properties. This calculation can be computationally expensive due to solution of the local problems in each coarse cell up to fine grid resolution of the heterogeneous fields. Next, we will describe the construction of the machine learning algorithm for the fast calculation. We will use presented properties calculation technique for creating a dataset for train and test a deep neural network.

4 Machine learning algorithm

In this section, we present a machine learning approach for solution of the stochastic poroelasticity problem. The main idea is to use different realizations of the permeability and elastic coefficient fields to train and test a deep neural network. After that, constructed deep network is used to fast and accurate solution of the coarse grid poroelasticity system.

We have following main steps:

- Generate dataset to train and test of the neural network.
- Construction of the neural network and test it on a set of realizations.
- Fast construction and solution of the coarse grid system using trained neural network for effective property prediction.

Next, we consider generation of the dataset and network construction in details.

4.1 Stochastic properties

We suppose isotropic permeability field and for elasticity tensor, we have

$$C = \begin{bmatrix} \lambda + 2\mu & \lambda & 0 \\ \lambda & \lambda + 2\mu & 0 \\ 0 & 0 & 2\mu \end{bmatrix}, \quad C = \begin{bmatrix} \lambda + 2\mu & \lambda & \lambda & 0 & 0 & 0 \\ \lambda & \lambda + 2\mu & \lambda & 0 & 0 & 0 \\ \lambda & \lambda & \lambda + 2\mu & 0 & 0 & 0 \\ 0 & 0 & 0 & 2\mu & 0 & 0 \\ 0 & 0 & 0 & 0 & 2\mu & 0 \\ 0 & 0 & 0 & 0 & 0 & 2\mu \end{bmatrix},$$

for 2D and 3D problems, respectively. Here for Lamé parameters, we have

$$\mu = \frac{E}{2(1+\eta)}, \quad \lambda = \frac{E\eta}{(1+\eta)(1-2\eta)}.$$

where $\eta = \text{const}$ is the Poisson's ratio.

Let $Y(x, \omega)$ is the random normal field generated by the Karhunen-Loève (KL) expansion with the corresponding covariance matrix $R(x, y)$ [1, 14]. We suppose that the Covariance structure $R(x, y)$ is of the form

$$R(x, y) = \sigma^2 \exp \left(- \sum_{i=1}^d \frac{|x_i - y_i|^2}{2l_i^2} \right), \quad (11)$$

where l_1, l_2, l_3 are the correlation lengths and σ^2 is the variance.

We have

$$Y(x, \omega) = \sum_{k=1}^{N_Y} \sqrt{\lambda_k} \nu_k(\omega) \varphi_k(x),$$

where ν_k is the stochastic coefficients, φ_k and λ_k are the eigenfunctions and eigenvalues .

The stochastic permeability and elastic modulus fields ($\kappa = \kappa(x, \omega)$, $E = E(x, \omega)$) are given as follows

$$k(x, \omega) = \exp(Y(x, \omega)), \quad E(x, \omega) = \bar{E}(x) + \alpha Y(x, \omega), \quad (12)$$

where $\alpha > 0$ is the strength of the randomness.

4.2 Dataset

We construct deep neural network, whereas input parameters we use a set of fine grid random properties in local domains and as output, we use an effective properties (k^* and C^*).

We have following steps:

- Generate a set of random realizations of $Y(x, \omega_l)$ ($l = \overline{1, M}$) and

$$k(x, \omega_l) = \exp(Y(x, \omega_l)), \quad E(x, \omega_l) = \bar{E}(x) + \alpha Y(x, \omega_l).$$

- Define a uniform $N \times N$ coarse grid $\mathcal{T}^H = \cup_i K_i$ with $i = \overline{1, N_c}$ and $N_c = N \cdot N$.
- For each realization $k(x, \omega_l)$:
 - Divide permeability into local domains, $k^{K_i}(x, \omega_l)$.
 - Calculate effective permeability tensor $k^{*, K_i}(\omega_l)$ by solution of the local problems in K_i .
- For each realization $E(x, \omega_l)$:
 - Divide elastic modulus into local domains, $E^{K_i}(x, \omega_l)$.
 - Calculate effective elasticity tensor C^{*, K_i} by solution of the local problems in K_i .
- Save $\{k^{K_i}(x, \omega_l) \rightarrow k^{*, K_i}(\omega_l)\}$ and $\{E^{K_i}(x, \omega_l) \rightarrow C^{*, K_i}(\omega_l)\}$ for $i = \overline{1, N_c}$ and $l = \overline{1, M}$.
- Normalize dataset and use it for machine learning algorithm construction.

We have two datasets: (1) 2D stochastic fields and (2) 3D stochastic fields. Each of the stochastic field is represented as d -dimensional array with size N_l^d ($d = 2, 3$), where each value represent normalized property of the heterogeneous media. The scale of each array in dataset are scaled to fall within the range 0 to 1. For representing heterogeneous properties, the high resolution representation should be used for better accuracy of the homogenization methods.

The input of the network is d - dimensional normalized array

$$X_j = k^{K_i}(x, \omega_l) \quad \text{or} \quad X_j = E^{K_i}(x, \omega_l), \quad j = l \cdot M + i, \quad i = \overline{1, N_c}, \quad l = \overline{1, M},$$

where X_j has size N_l^d and $j = \overline{1, L}$ is the size of the dataset, where $L = M \cdot N_c$.

The output for the numerical homogenization is the normalized array of the effective properties

$$Y_j = k^{*, K_i}(\omega_l) \quad \text{or} \quad Y_j = C^{*, K_i}(\omega_l), \quad j = l \cdot M + i, \quad i = \overline{1, N_c}, \quad l = \overline{1, M},$$

where k^{*, K_i} and C^{*, K_i} are tensors that represented as array with symmetric property.

The dataset $\{X_j \rightarrow Y_j\}$ with $j = \overline{1, L}$ contains $L = N_c \cdot M$ local stochastic fields and used to train, validate and test the neural network. In general, effective properties (output) can be obtained from laboratory measurement and input dataset can be obtained using high resolution tomography [28, 30, 8]. For example for permeability calculation, digital rock database can be used.

4.3 Network

In recent years, many new highly effective methods for constructing artificial intelligence have appeared. This jump is associated with the development of new methods based on the construction of deep learning methods through convolutional neural networks, and the development of open source libraries that accelerate calculations on GPUs. The architecture of a convolutional neural network (CNN) contains composing of the convolutional and pooling layers that passed through a non-linearity such as a ReLU functions [21, 20]. Several layers of convolution, non-linearity and pooling are stacked, and completes with a several fully-connected layers.

We train a convolutional neural network by a dataset $\{X_j \rightarrow Y_j\}$ of local random coefficients (X_j) and macroscale characteristics (effective medium properties, Y_j). Constructed machine learning algorithm efficiently determine of dependencies and used for fast calculation of a effective properties of random media.

To generate a dataset for machine learning, the samples X_j are generated randomly and to compute train set Y_j , we use numerical homogenization

$$\{X_1, ..., X_i, ..., X_N\} \rightarrow \text{Numerical homogenization} \rightarrow \{Y_1, ..., Y_i, ..., Y_N\}.$$

Next, we divide dataset into train, validation and test sets with sizes N_{train} , N_{val} and N_{test} . As test set, we take 60 % of data, another 40 % randomly divided between train and validation set in 80/20 proportion. Therefore, following dataset is used for train convolutional neural network (CNN)

$$\text{Train set: } \{(X_1, Y_1), ..., (X_i, Y_i), ..., (X_{N_{train}}, Y_{N_{train}})\} \rightarrow \text{CNN}$$

We use validation set to validate a training process and test data for testing constructed machine learning algorithm. After that we use the constructed network as a “black box” for fast prediction of the effective properties for a given local heterogeneity:

$$X \rightarrow \text{CNN} \rightarrow Y.$$

Convolutional neural network is the deep neural network with multiple layers that compute a function $F(X_i, W)$, where X_i is the input data and W is the system parameters. By a training process, a machine learning algorithm solve the optimization problem to find model weights that best describe the train set by minimization of the loss function. In this work, we use the mean square error (MSE) as a loss function

$$E_{train} = \frac{1}{N_{train}} \sum_{i=1}^{N_{train}} |Y_i - F(X_i, W)|^2$$

and also calculate validation set loss function. For solution of the minimization problem, we use gradient-based optimizer Adam [18].

The convolutional neural network has several convolutional and pooling layers with rectified linear units (RELU) activation layer, and two fully connected layers with Dropout. Dropout algorithm consists of randomly dropping out units of the network during the optimization iteration. Convolution layers extract and combine local features in d - dimensional arrays due to convolution process that alternates with pooling layers for reduction of the spatial resolution. The pooling layer perform a local averaging. Several layers of convolutions and pooling are alternated in order to detect higher order features for better accuracy of the method. Successive layers of convolutions and pooling are alternated. Finally, several fully connected layers are applied.

5 Results

The numerical calculations of the effective properties has been implemented with the open-source finite element software FEniCS [23]. Implementation of the machine learning method is based on the open source library Keras [9]. Keras is a open-source library that provide high-level building blocks for developing deep-learning models and based on the several backend engines. We use TensorFlow backend [2].

We consider three test cases with different KL-expansion parameters for dataset generation:

Test 1. 2D problem with $l_1^2 = 0.2$, $l_2^2 = 0.2$ and $\sigma^2 = 2$.

Test 2. 2D problem with $l_1^2 = 0.1$, $l_2^2 = 0.4$ and $\sigma^2 = 2$.

Test 3. 3D problem with $l_1^2 = 0.2$, $l_2^2 = 0.2$, $l_3^2 = 0.2$ and $\sigma^2 = 2$.

At first, we present results for numerical homogenization method for poroelasticity problem in the stochastic media and compare errors between coarse grid solution and reference (fine grid) solutions. Next, we present results for the machine learning algorithm and calculate errors for train and test datasets. Finally, we consider a coarse grid solution of the problem, where effective properties are calculated using constructed machine learning method and discuss computational efficiency of the presented method.

5.1 Numerical homogenization results

In this section, we present numerical results of the numerical homogenization method for poroelasticity problems in heterogeneous media. For poroelastic problem, we set $\alpha = 1$ and $M = 1$. As initial conditions, we set $p_0 = 0$ and perform calculations for $T_{max} = 0.001$ with 20 time steps. We perform calculations using structured coarse and fine grids. For each test problems, we consider three cases by varying a heterogeneous elasticity modulus and permeability.

Two-dimensional problem (Tests 1 and 2). We solve poroelasticity problem in $\Omega = [0, 1] \times [0, 1]$. We set following boundary conditions

$$\begin{aligned} u_1 &= 0, & \sigma_2 &= 0, & x &\text{ on } \Gamma_L \\ \sigma_1 &= 0, & u_2 &= 0, & x &\text{ on } \Gamma_B \\ p &= 1, & x &\text{ on } \Gamma_T. \end{aligned}$$

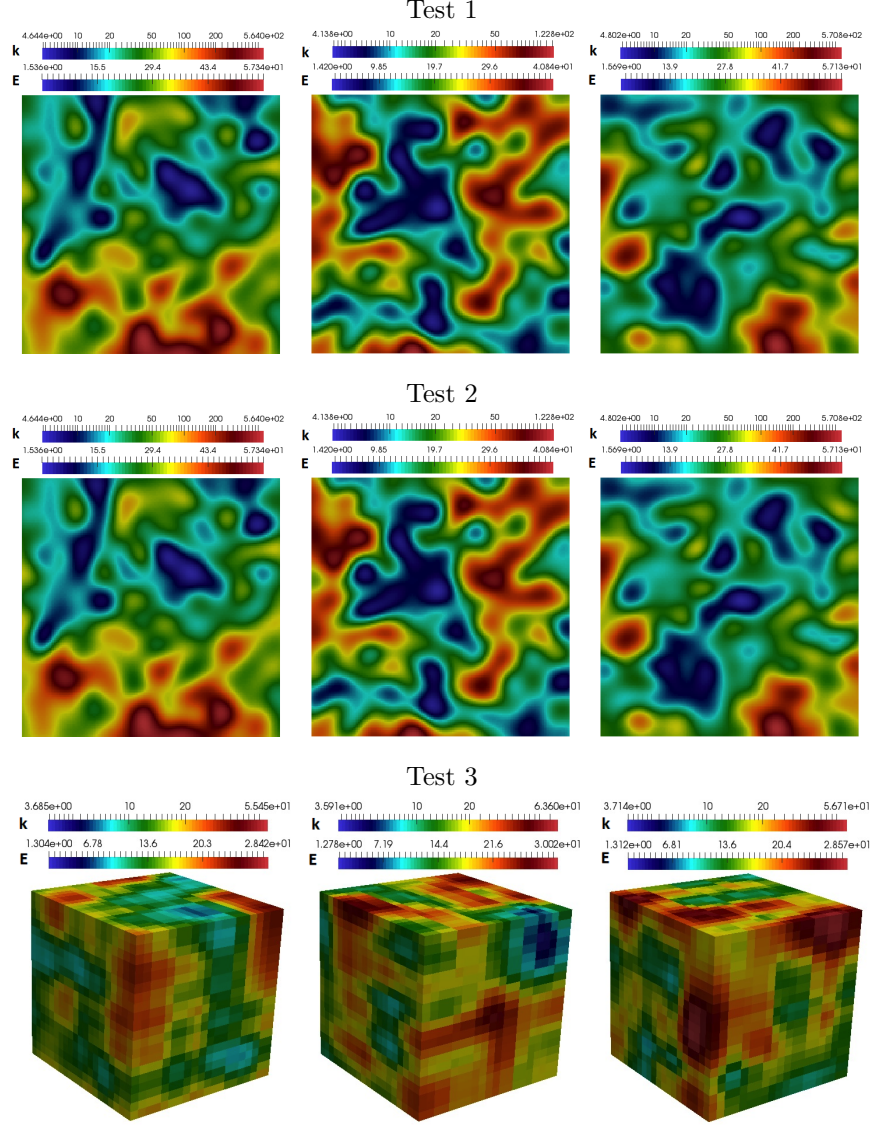


Figure 1: Heterogeneous elasticity modulus and permeability. First row: Cases 1, 2 and 3 (from left to right) for Test 1. Second row: Cases 1, 2 and 3 (from left to right) for Test 2. Third row: Cases 1, 2 and 3 (from left to right) for Test 3.

where Γ_L and Γ_R are the left and right boundaries, Γ_B and Γ_T are the bottom and top boundaries, $\partial\Omega = \Gamma_L \cup \Gamma_R \cup \Gamma_B \cup \Gamma_T$.

Three-dimensional problem (Test 3). We solve model problem in $\Omega = [0, 1] \times [0, 1] \times [0, 1]$. We set

Case	$\ e_p\ _1$ (%)	$\ e_p\ _2$ (%)	$\ e_u\ _1$ (%)	$\ e_u\ _2$ (%)
Test 1				
1	2.86139	16.3882	8.84006	16.2718
2	3.4038	15.8993	9.21494	15.9281
3	2.82176	12.7992	8.56077	14.3118
Test 2				
1	3.917	11.497	3.644	12.433
2	3.721	11.842	3.995	9.544
3	2.939	10.849	3.712	10.216
Test 3				
1	7.923	20.993	8.607	24.203
2	7.385	21.724	7.475	19.563
3	7.223	21.603	5.399	21.777

Table 1: Relative L_2 and energy errors for displacement and pressure between coarse grid solution and reference solution. Tests 1, 2 and 3 with three cases

following boundary conditions

$$\begin{aligned}
u_1 &= 0, & \sigma_2 &= 0, & \sigma_3 &= 0, & x &\text{ on } \Gamma_L \\
\sigma_1 &= 0, & u_2 &= 0, & \sigma_3 &= 0, & x &\text{ on } \Gamma_B \\
\sigma_1 &= 0, & \sigma_2 &= 0, & u_3 &= 0, & x &\text{ on } \Gamma_W \\
p &= 1, & x &\text{ on } \Gamma_T.
\end{aligned}$$

where Γ_L and Γ_R are the left and right boundaries, Γ_B and Γ_T are the bottom and top boundaries, Γ_F and Γ_W are the forward and backward boundaries, $\partial\Omega = \Gamma_L \cup \Gamma_R \cup \Gamma_B \cup \Gamma_T \cup \Gamma_F \cup \Gamma_W$.

We compute relative L_2 and energy errors between fine grid (reference) solution (p_f, u_f) and coarse grid solution (p, u)

$$\begin{aligned}
\|e_p\|_1^2 &= \frac{\int_{\Omega} (p_f - p)^2 dx}{\int_{\Omega} p_f dx}, & \|e_u\|_1^2 &= \frac{\int_{\Omega} (u_f - u)^2 dx}{\int_{\Omega} u_f^2 dx}, \\
\|e_p\|_2^2 &= \frac{\int_{\Omega} k \nabla(p_f - p) \cdot \nabla(p_f - p) dx}{\int_{\Omega} k \nabla(p_f) \cdot \nabla(p_f) dx}, & \|e_u\|_2^2 &= \frac{\int_{\Omega} \sigma(u_f - u) : \varepsilon(u_f - u) dx}{\int_{\Omega} \sigma(u_f) : \varepsilon(u_f) dx}.
\end{aligned}$$

We consider three test cases for different heterogeneity (see Figure 1) for Tests 1, 2 and 3. For 2D problems (Tests 1 and 2), coarse grid is 10×10 and fine grid is 320×320 . For 3D problems (Test 3), coarse grid is $5 \times 5 \times 5$ and fine grid is $60 \times 60 \times 60$. In Table 1, we present the relative L_2 and energy errors of the coarse grid solver for Tests 1, 2 and 3. We observe good accuracy for both 2D and 3D test problems with different heterogeneity. Next, we consider a machine learning technique for fast prediction of the effective properties for Tests 1, 2 and 3.

5.2 Results of the learning process

For dataset construction, we generate a set of random realizations $Y(x, \omega_l)$ ($l = \overline{1, M}$) and construct

$$k(x, \omega_l) = \exp(Y(x, \omega_l)), \quad E(x, \omega_l) = \bar{E}(x) + \alpha Y(x, \omega_l).$$

Next, we define a uniform $N \times N$, divide $k(x, \omega_l) = \cup_i k^{K_i}(x, \omega_l)$ and $E(x, \omega_l) = \cup_i E^{K_i}(x, \omega_l)$ into local domains K_i , where $i = \overline{1, N_c}$ and $N_c = N \cdot N$.

Then for each $k^{K_i}(x, \omega_l)$ and $E^{K_i}(x, \omega_l)$ using numerical homogenization technique, we calculate $\{k^{K_i}(x, \omega_l) \rightarrow k^{*, K_i}(\omega_l)\}$ and $\{E^{K_i}(x, \omega_l) \rightarrow C^{*, K_i}(\omega_l)\}$ for $i = \overline{1, N_c}$ and $l = \overline{1, M}$. Finally, we normalize dataset and use it for machine learning algorithm construction (each component of the effective tensor is normalized separately).

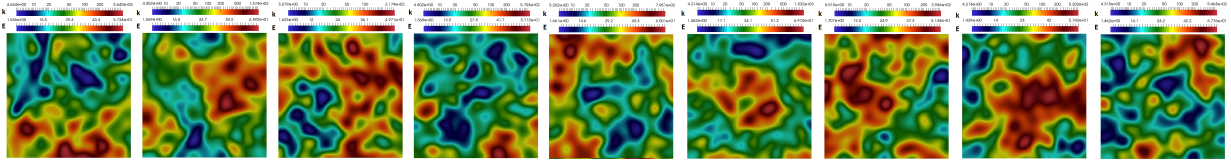


Figure 2: Dataset for 2D problem. Test 1

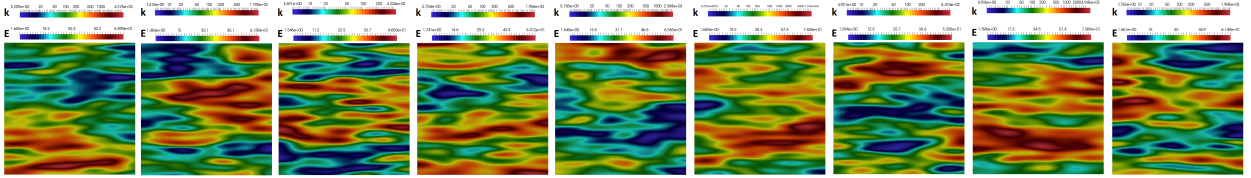


Figure 3: Dataset for 2D problem. Test 2

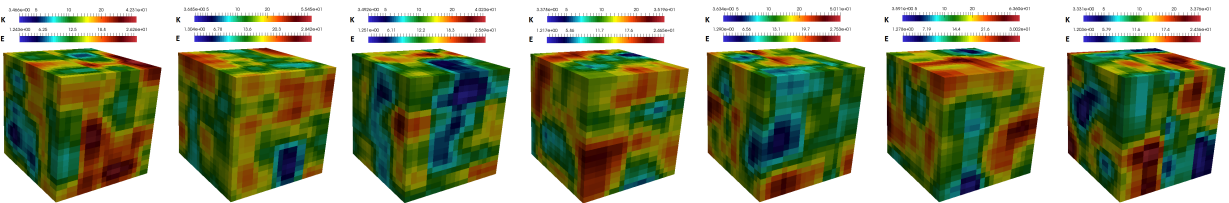


Figure 4: Dataset for 3D problem. Test 3

We set $M = 100$, $N = 10$ for 2D problems and $N = 5$ for 3D problem. Therefore, we have dataset with size $L = 100 \cdot 10^2$ (for Tests 1 and for Test 2, separately) and $L = 100 \cdot 5^3$ (Test 3). Therefore input of the network is d - dimensional normalized array

$$X_j = k^{K_i}(x, \omega_l) \quad \text{or} \quad X_j = E^{K_i}(x, \omega_l), \quad j = l \cdot M + i,$$

where X_j has size N_l^d , where $N_l = 64$ (Tests 1 and 2) and $N_l = 12$ (Test 3).

Input: train and validation set ($i = 1, \dots, (N_{train} + N_{val})$)	$K_i^{N_l \times N_l}$
2D Convolution with L_1 filters with (3, 3) - kernel and RELU activation	$L_1 \times K_i^{N_l \times N_l}$
Max pooling with (2, 2) - kernel	$L_1 \times K_i^{N_l/2 \times N_l/2}$
2D Convolution with L_2 filters with (3, 3) - kernel and RELU activation	$L_2 \times K_i^{N_l/2 \times N_l/2}$
Max pooling with (2, 2) - kernel	$L_2 \times K_i^{N_l/4 \times N_l/4}$
2D Convolution with L_3 filters with (3, 3) - kernel and RELU activation	$L_3 \times K_i^{N_l/4 \times N_l/4}$
Max pooling with (2, 2) - kernel	$L_3 \times K_i^{N_l/8 \times N_l/8}$
2D Convolution with L_4 filters with (3, 3) - kernel and RELU activation	$L_4 \times K_i^{N_l/8 \times N_l/8}$
Max pooling with (2, 2) - kernel	$L_4 \times K_i^{N_l/16 \times N_l/16}$
Fully connected layer with dropout	$L_2 \times N_l/16 \times N_l/16$
Fully connected layer with dropout	L_5
Output	N_{out}

Table 2: Convolutional neural network architecture for prediction effective properties. $N_l = 64$, $L_1 = 8$, $L_2 = 16$, $L_3 = 32$, $L_4 = 64$, $L_5 = 512$, $N_{out} = 3$ for effective permeability prediction and $N_{out} = 6$ for elasticity tensor. 2D problem.

Input: train and validation set ($i = 1, \dots, (N_{train} + N_{val})$)	$K_i^{N_l \times N_l \times N_l}$
3D Convolution with L_1 filters with (3, 3, 3) - kernel and RELU activation	$L_1 \times K_i^{N_l \times N_l \times N_l}$
Max pooling with (2, 2, 2) - kernel	$L_1 \times K_i^{N_l/2 \times N_l/2 \times N_l/2}$
3D Convolution with L_2 filters with (3, 3, 3) - kernel and RELU activation	$L_2 \times K_i^{N_l/2 \times N_l/2 \times N_l/2}$
Max pooling with (2, 2, 2) - kernel	$L_2 \times K_i^{N_l/4 \times N_l/4 \times N_l/4}$
Fully connected layer with dropout	$L_2 \times N_l/4 \times N_l/4 \times N_l/4$
Fully connected layer with dropout	L_3
Output	N_{out}

Table 3: Convolutional neural network architecture for prediction effective properties. $N_l = 12$, $L_1 = 16$, $L_2 = 32$, $L_3 = 512$, $N_{out} = 6$ for effective permeability prediction and $N_{out} = 21$ for elasticity tensor. 3D problem.

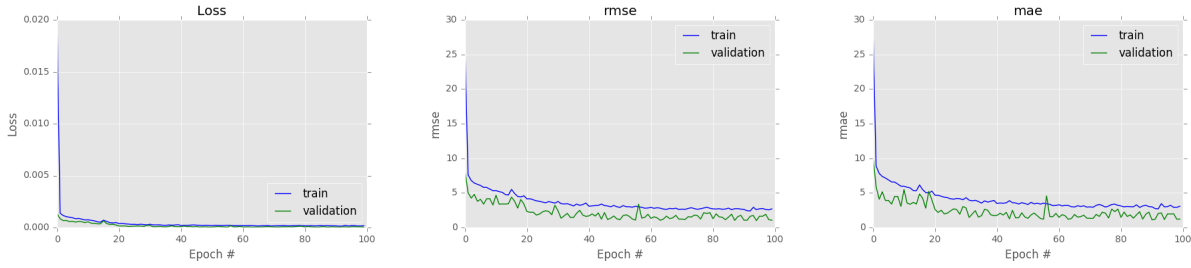


Figure 5: Learning process for Test 1. Loss, relative root mean square error and relative mean absolute error vs epoch number for numerical homogenization. Effective permeability tensor for Test 1

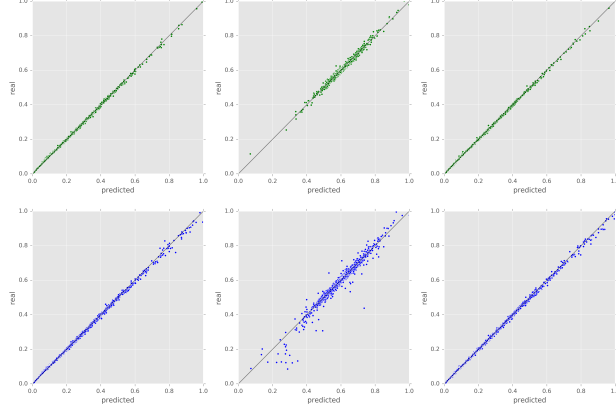


Figure 6: Learning performance of CNN for 2D problem (Test 1). Effective permeability tensor, $Y_i = \{k_{11}^{*,K_i}, k_{12}^{*,K_i}, k_{22}^{*,K_i}\}$ (from left to right). Parity plots comparing preference property values against predictions made using CNN. First row: train and validation dataset (green color). Second row: test dataset (blue color)

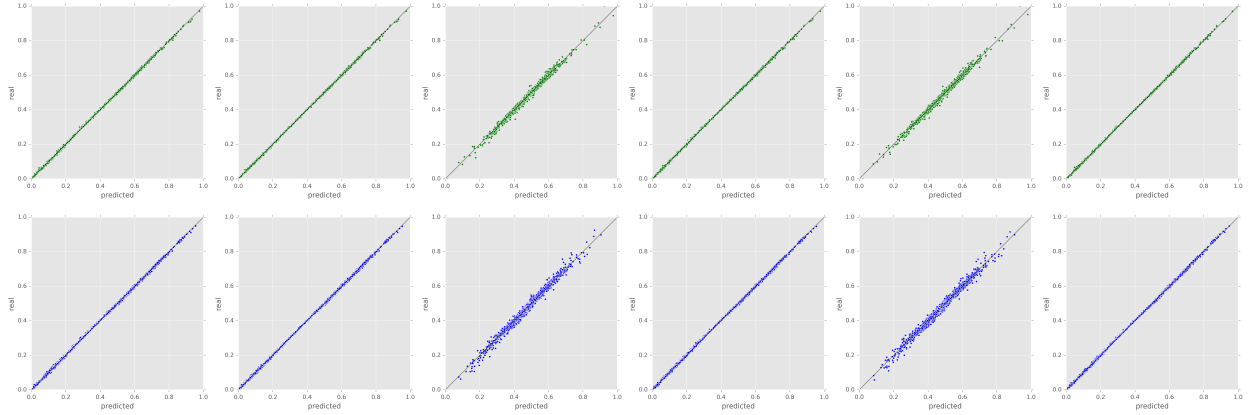


Figure 7: Learning performance of CNN for 2D problem (Test 1). Effective elasticity tensor, $Y_i = \{C_{1111}^{*,K_i}, C_{1122}^{*,K_i}, C_{1112}^{*,K_i}, C_{2222}^{*,K_i}, C_{2212}^{*,K_i}, C_{1212}^{*,K_i}\}$ (from left to right). Parity plots comparing preference property values against predictions made using CNN. First row: train and validation dataset (green color). Second row: test dataset (blue color)

The output for the numerical homogenization is the normalized array of the effective properties

$$Y_j = k^{*,K_i}(x, \omega_l) \quad \text{or} \quad Y_j = C^{*,K_i}(x, \omega_l), \quad j = l \cdot M + i, \quad i = \overline{1, N_c}, \quad l = \overline{1, M},$$

where k^{*,K_i} and C^{*,K_i} are tensors that represented as array with symmetric property.

The dataset $\{X_j \rightarrow Y_j\}$ used to train, validate and test the neural network (see Figures 2, 3 and 4 for illustration of $k(x, \omega_l)$ and $E(x, \omega_l)$). Each dataset is divided into 3200:800:6000 ratio for training, validation and test sets.

For calculations, we use 100 epochs with a batch size N_c (number of coarse cells) and Adam optimizer with

Error	Train set			Test set		
	MSE	RMSE (%)	MAE (%)	MSE	RMSE (%)	MAE (%)
effective permeability tensor						
k_{11}	0.047	2.190	2.436	0.059	2.446	2.413
k_{12}	0.012	1.131	0.834	0.074	2.730	1.083
k_{22}	0.040	2.013	2.248	0.051	2.279	2.254
k	0.016	1.290	1.218	0.071	2.671	1.436
effective elasticity tensor						
C_{1111}	0.008	0.903	0.788	0.008	0.942	0.819
C_{1122}	0.007	0.853	0.756	0.007	0.893	0.795
C_{1112}	0.026	1.625	1.177	0.033	1.840	1.292
C_{2222}	0.008	0.931	0.832	0.009	0.965	0.867
C_{2212}	0.025	1.602	1.175	0.034	1.848	1.303
C_{1212}	0.006	0.810	0.695	0.007	0.853	0.728
C	0.015	1.242	0.929	0.019	1.287	0.998

Table 4: Learning performance of CNN for 2D problem. Errors for Test 1

Error	Train set			Test set		
	MSE	RMSE (%)	MAE (%)	MSE	RMSE (%)	MAE (%)
effective permeability tensor						
k_{11}	0.101	3.191	2.791	0.112	3.350	2.744
k_{12}	0.091	3.019	1.516	0.246	4.960	1.962
k_{22}	0.168	4.110	3.634	0.290	5.387	3.701
k	0.094	3.081	1.874	0.238	4.885	2.282
effective elasticity tensor						
C_{1111}	0.010	1.014	0.836	0.010	1.015	0.815
C_{1122}	0.010	1.002	0.845	0.009	0.988	0.819
C_{1112}	0.075	2.745	2.048	0.092	3.039	2.128
C_{2222}	0.009	0.988	0.806	0.009	0.988	0.796
C_{2212}	0.072	2.682	1.922	0.085	2.932	1.973
C_{1212}	0.009	0.971	0.804	0.009	0.978	0.788
C	0.035	1.888	1.268	0.039	1.987	1.261

Table 5: Learning performance of CNN for 2D problem. Errors for Test 2

learning rate $\epsilon = 0.001$. For accelerating of the training process of the CNN, we use GPU (Nvidia GeForce GTX 1080 Ti). In order to prevent overfitting, we use dropout with rate 10 %. We use d - dimensional convolutions and max pooling layers with size 3^d and 2^d , respectively. The architectures of the CNN for 2D

Error	Train set			Test set		
	MSE	RMSE (%)	MAE (%)	MSE	RMSE (%)	MAE (%)
effective permeability tensor						
k_{11}	0.027	1.644	1.191	0.041	2.039	1.287
k_{22}	0.021	1.468	1.108	0.049	2.235	1.263
k_{33}	0.025	1.586	1.181	0.051	2.274	1.329
k_{12}	0.040	2.003	1.262	0.118	3.446	1.603
k_{13}	0.050	2.238	1.351	131	3.629	1.642
k_{23}	0.036	1.904	1.372	0.207	4.559	1.800
k	0.039	1.991	1.283	0.132	3.646	1.567
effective elasticity tensor						
C_{1111}	0.017	1.337	1.063	0.020	1.434	1.096
C_{1122}	0.016	1.269	1.015	0.018	1.343	1.042
C_{1133}	0.016	1.272	1.004	0.019	1.381	1.047
C_{1112}	0.055	2.361	1.675	0.079	2.823	1.926
C_{1123}	0.028	1.702	1.172	0.052	2.299	1.435
C_{1131}	0.039	1.985	1.420	0.059	2.447	1.630
C_{2222}	0.014	1.189	0.923	0.016	1.282	0.960
C_{2233}	0.014	1.216	0.973	0.017	1.307	1.007
C_{2212}	0.049	2.220	1.559	0.074	2.735	1.811
C_{2223}	0.031	1.781	1.251	0.056	2.378	1.524
C_{2231}	0.038	1.950	1.373	0.058	2.418	1.584
C_{3333}	0.015	1.262	0.981	0.018	1.375	1.028
C_{3312}	0.051	2.261	1.593	0.079	2.813	1.854
C_{3323}	0.027	1.664	1.149	0.050	2.256	1.419
C_{3331}	0.038	1.966	1.394	0.059	2.444	1.603
C_{1212}	0.017	1.309	1.013	0.020	1.418	1.055
C_{1223}	0.059	2.429	1.717	0.085	2.929	1.933
C_{1231}	0.042	2.070	1.469	0.073	2.716	1.780
C_{2323}	0.014	1.218	0.958	0.017	1.318	0.989
C_{2331}	0.081	2.853	2.009	0.115	3.396	2.275
C_{3131}	0.015	1.229	0.995	0.017	1.331	1.027
C	0.033	1.838	1.286	0.050	2.255	1.452

Table 6: Learning performance of CNN for 3D problem. Errors for Test 3

and 3D problems are presented in Tables 2 and 3. Proposed CNN for 2D problems contains 11 layers and 7 layers for 3D problems. The input data X_i is a N_l^d array with $d = 2, 3$, $N_l = 64$ for 2D and $N_l = 12$ for 3D. Convolution layer contains L_i feature maps. Finally, we apply three fully connected layers.

For error calculation on the train and test dataset, we use mean square errors, relative mean absolute and relative root mean square errors

$$MSE = \sum_i |Y_i - \tilde{Y}_i|^2, \quad MAE = \frac{\sum_i |Y_i - \tilde{Y}_i|}{\sum_i |Y_i|}, \quad RMSE = \sqrt{\frac{\sum_i |Y_i - \tilde{Y}_i|^2}{\sum_i |Y_i|^2}},$$

where Y_i and \tilde{Y}_i denotes the reference and predicted values for sample X_i

Convergence of the loss function for Test 1 (2D) is presented in Figure 5, where we plot the relative root mean square error (RMSE) and relative mean absolute error (MAE) vs epoch number. We depict loss functions for train and validation sets for learning of the effective permeability tensor. In Figures 6 and 7, we present a parity plots comparing preference property values against predicted using CNN. Learning performance of CNN for 2D and 3D problems are presented in Tables 4, 7 and 6 for Tests 1, 2 and 3, respectively. We observe good convergence for the relative errors for train and test sets.

5.3 Numerical homogenization with machine learning approach

Next, we consider errors between solution of the coarse grid problem with reference and predicted effective properties. We present results for the Tests 1, 2 and 3.

Test	Offline (GPU)	Online (loading)	Online (prediction)	Direct solve	Speedup
effective permeability tensor					
Test 1 (2D)	40.688	0.547	0.171	13.025	× 76.1
Test 2 (2D)	40.798	0.580	0.171	13.025	× 76.1
Test 3 (3D)	41.163	0.431	0.552	44.833	× 81.2
effective elasticity tensor					
Test 1 (2D)	42.807	0.485	0.171	23.333	× 136.4
Test 2 (2D)	47.169	0.433	0.173	23.333	× 134.8
Test 3 (3D)	41.789	0.484	0.532	153.82	× 289.1

Table 7: Time in seconds. Offline time is the time of CNN training and validation on GPU. Online calculations contains neural network loading and prediction of the coarse grid effective properties for one Ω . Direct solve is the time of effective properties calculation for one Ω . Speedup is Direct solve/Online (prediction)

In Figure 8, we present results for numerical homogenization for 100 samples of the random field. We depict a relative mean square error in percentages for pressure and displacements with effective coefficients predicted using machine learning algorithm for Test 1, 2 and 3. We observe small errors (near one percent) with fast calculations using a machine learning algorithm.

Finally, we discuss the computational gain of the machine learning method that achieved by the fast calculations of the effective properties and local matrices. We divide calculation on the offline and online stages for machine learning algorithm. On the online stage, we train neural network on the GPU by a given train and validation datasets. We note that, here we didn't consider time of the dataset construction. On

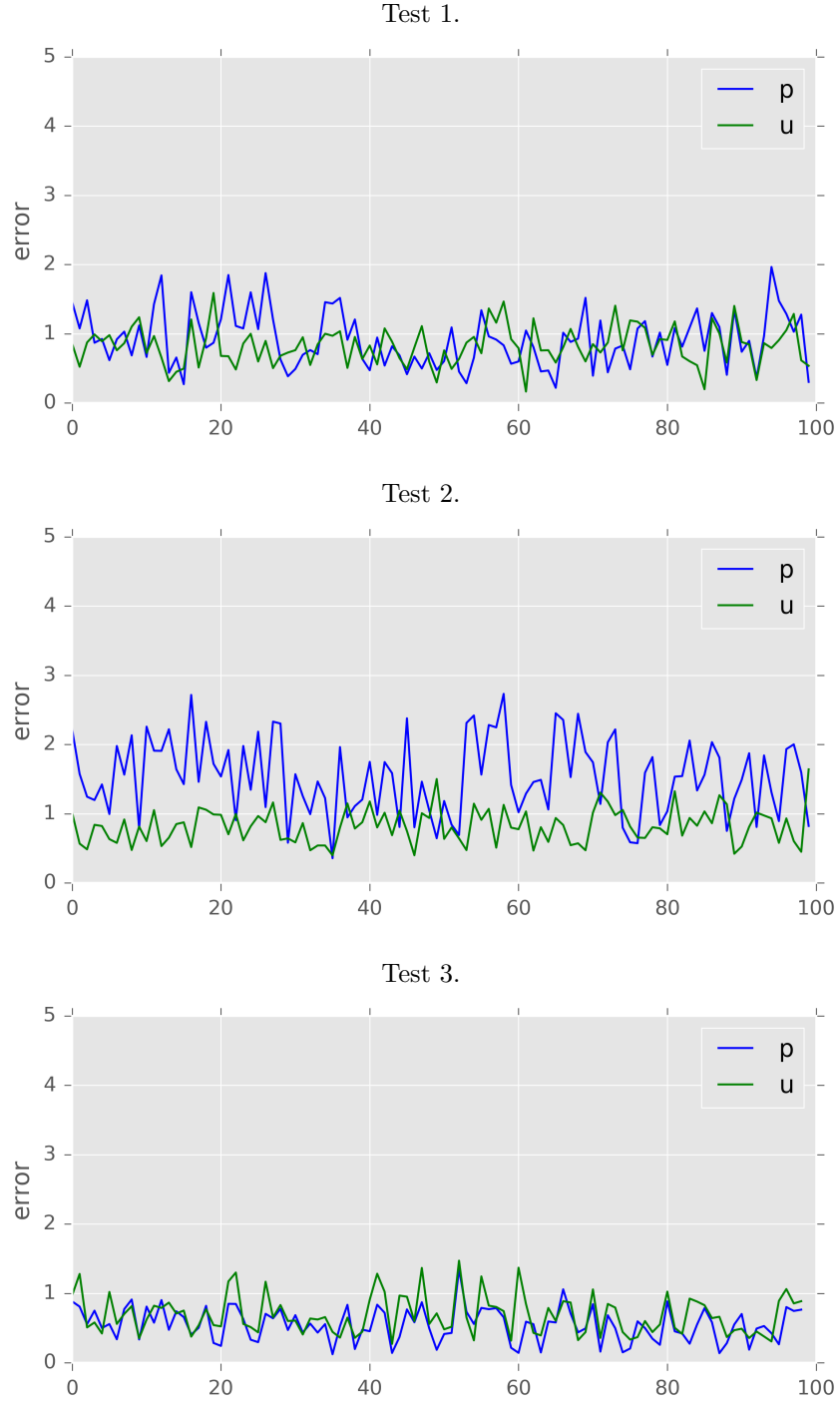


Figure 8: Numerical homogenization error with effective coefficients predicted using machine learning algorithm. Test 1, 2 and 3 (from top to bottom). Pressure (blue) and displacement (green)

the offline stage, we have two steps: loading of the preconstructed neural network and prediction of the effective properties for a given fine scale distribution. We compare time of the prediction vs time of direct solution of the local problems for effective properties calculations for a some givens fine scale properties in domain Ω .

We observe high speedup of the calculations using GPU. Time is 1574.910 seconds if we train the neural network on CPU (2.9 GHz Intel Core i5) and 13.025 seconds on GPU for Test 1 (effective permeability tensor). Therefore, we obtain $\times 38$ faster neural network construction on the GPU (Nvidia GeForce GTX 1080Ti). In Table 7, we present time of offline and online stages. On the table, we depict the offline calculation speedup using direct simulations and prediction using CNN. We have approximately $\times 80$ faster calculations for effective permeability and $\times (130 - 290)$ faster for effective elasticity tensor.

6 Conclusion

In this work, we considered a numerical homogenization of the poroelasticity problem with stochastic properties. For accelerating of the calculations of the effective properties, we constructed a machine learning algorithm. We constructed a machine learning algorithm through convolutional neural network (CNN) to learn a map between input stochastic fields to effective properties. We trained neural network on the set of the selected realizations of the local microscale stochastic fields and macroscale characteristics (permeability and elasticity tensors). Proposed method is used to make fast and accurate effective property predictions for numerical solution of the poroelasticity problems in stochastic media.

References

- [1] Jørg E Aarnes and Yalchin Efendiev. Mixed multiscale finite element methods for stochastic porous media flows. *SIAM Journal on Scientific Computing*, 30(5):2319–2339, 2008.
- [2] Martín Abadi, Paul Barham, Jianmin Chen, Zhifeng Chen, Andy Davis, Jeffrey Dean, Matthieu Devin, Sanjay Ghemawat, Geoffrey Irving, Michael Isard, et al. Tensorflow: a system for large-scale machine learning. In *OSDI*, volume 16, pages 265–283, 2016.
- [3] I Yucel Akkutlu, Yalchin Efendiev, Maria Vasilyeva, and Yuhe Wang. Multiscale model reduction for shale gas transport in poroelastic fractured media. *Journal of Computational Physics*, 353:356–376, 2018.
- [4] Grégoire Allaire. Homogenization and two-scale convergence. *SIAM Journal on Mathematical Analysis*, 23(6):1482–1518, 1992.
- [5] NS Bakhvalov and GP Panasenko. Homogenization in periodic media, mathematical problems of the mechanics of composite materials. *ed: Nauka, Moscow*, 1984.
- [6] Donald L Brown and Maria Vasilyeva. A generalized multiscale finite element method for poroelasticity problems i: linear problems. *Journal of Computational and Applied Mathematics*, 294:372–388, 2016.

- [7] Donald L Brown and Maria Vasilyeva. A generalized multiscale finite element method for poroelasticity problems ii: Nonlinear coupling. *Journal of Computational and Applied Mathematics*, 297:132–146, 2016.
- [8] Shing Chan and Ahmed H Elsheikh. A machine learning approach for efficient uncertainty quantification using multiscale methods. *Journal of Computational Physics*, 354:493–511, 2018.
- [9] François Chollet et al. Keras: Deep learning library for theano and tensorflow. URL: <https://keras.io/>.
- [10] Régis Cottureau. Numerical strategy for unbiased homogenization of random materials. *International Journal for Numerical Methods in Engineering*, 95(1):71–90, 2013.
- [11] Olivier Coussy. *Poromechanics*. John Wiley & Sons, 2004.
- [12] Paul Dostert, Yalchin Efendiev, Thomas Y Hou, and Wuan Luo. Coarse-gradient langevin algorithms for dynamic data integration and uncertainty quantification. *Journal of computational physics*, 217(1):123–142, 2006.
- [13] Yalchin Efendiev, Juan Galvis, and Florian Thomines. A systematic coarse-scale model reduction technique for parameter-dependent flows in highly heterogeneous media and its applications. *Multiscale Modeling & Simulation*, 10(4):1317–1343, 2012.
- [14] Benjamin Ganis, Hector Klie, Mary F Wheeler, Tim Wildey, Ivan Yotov, and Dongxiao Zhang. Stochastic collocation and mixed finite elements for flow in porous media. *Computer methods in applied mechanics and engineering*, 197(43-44):3547–3559, 2008.
- [15] S Hazanov and C Huet. Order relationships for boundary conditions effect in heterogeneous bodies smaller than the representative volume. *Journal of the Mechanics and Physics of Solids*, 42(12):1995–2011, 1994.
- [16] Xinguang He, Lijian Jiang, and J David Moulton. A stochastic dimension reduction multiscale finite element method for groundwater flow problems in heterogeneous random porous media. *Journal of hydrology*, 478:77–88, 2013.
- [17] J Kim, HA Tchelepi, and R Juanes. Stability and convergence of sequential methods for coupled flow and geomechanics: Drained and undrained splits. *Computer Methods in Applied Mechanics and Engineering*, 200(23):2094–2116, 2011.
- [18] Diederik P Kingma and Jimmy Ba. Adam: A method for stochastic optimization. *arXiv preprint arXiv:1412.6980*, 2014.
- [19] AE Kolesov, Petr N Vabishchevich, and Maria V Vasilyeva. Splitting schemes for poroelasticity and thermoelasticity problems. *Computers & Mathematics with Applications*, 67(12):2185–2198, 2014.
- [20] Alex Krizhevsky, Ilya Sutskever, and Geoffrey E Hinton. Imagenet classification with deep convolutional neural networks. In *Advances in neural information processing systems*, pages 1097–1105, 2012.

- [21] Yann LeCun, Yoshua Bengio, and Geoffrey Hinton. Deep learning. *nature*, 521(7553):436, 2015.
- [22] Yann LeCun, Léon Bottou, Yoshua Bengio, and Patrick Haffner. Gradient-based learning applied to document recognition. *Proceedings of the IEEE*, 86(11):2278–2324, 1998.
- [23] Anders Logg, Kent-Andre Mardal, and Garth Wells. *Automated solution of differential equations by the finite element method: The FEniCS book*, volume 84. Springer Science & Business Media, 2012.
- [24] Fanny Moravec and Sophie Roman. Numerical computing of elastic homogenized coefficients for periodic fibrous tissue. *Applied and Computational Mechanics*, 3(1):141–152, 2009.
- [25] Ghanshyam Pilania, Chenchen Wang, Xun Jiang, Sanguthevar Rajasekaran, and Ramamurthy Ramprasad. Accelerating materials property predictions using machine learning. *Scientific reports*, 3:2810, 2013.
- [26] Enrique Sánchez-Palencia. Non-homogeneous media and vibration theory. In *Non-homogeneous media and vibration theory*, volume 127, 1980.
- [27] Karen Simonyan and Andrew Zisserman. Very deep convolutional networks for large-scale image recognition. *arXiv preprint arXiv:1409.1556*, 2014.
- [28] Nattavadee Srisutthiyakorn. Deep learning methods for predicting permeability from 2-d/3-d binary segmented images. In *SEG International Exposition and 86th Annual Meeting, Dallas, Texas, USA*, pages 16–21, 2016.
- [29] Nitish Srivastava, Geoffrey Hinton, Alex Krizhevsky, Ilya Sutskever, and Ruslan Salakhutdinov. Dropout: a simple way to prevent neural networks from overfitting. *The Journal of Machine Learning Research*, 15(1):1929–1958, 2014.
- [30] Oleg Sudakov, Evgeny Burnaev, and Dmitry Koroteev. Driving digital rock towards machine learning: predicting permeability with gradient boosting and deep neural networks. *arXiv preprint arXiv:1803.00758*, 2018.
- [31] Alexey Talonov and Maria Vasilyeva. On numerical homogenization of shale gas transport. *Journal of Computational and Applied Mathematics*, 301:44–52, 2016.
- [32] Maria Vasilyeva, Eric T Chung, Yalchin Efendiev, and Jihoon Kim. Constrained energy minimization based upscaling for coupled flow and mechanics. *arXiv preprint arXiv:1805.09382*, 2018.
- [33] Maria Vasilyeva and Denis Stalnov. A generalized multiscale finite element method for thermoelasticity problems. In *International Conference on Numerical Analysis and Its Applications*, pages 713–720. Springer, 2016.